Liquid–Liquid Phase Separation and Crystallization in Thin Films of a Polyolefin Blend

Song Hong,[†,§] Xiaohua Zhang,[†] Ruoyu Zhang,[†,§] Li Wang,[†] Jiang Zhao,*[,†] and Charles C. Han*[,†]

State Key Laboratory of Polymer Physics and Chemistry, Joint Laboratory of Polymer Science and Materials, Beijing National Laboratory for Molecular Sciences, Institute of Chemistry, CAS, Beijing 100080, China, and Graduate University of Chinese Academy of Sciences, Beijing 100080, China

Received November 14, 2007
Revised Manuscript Received February 28, 2008

Polyolefins is one of the most important and widely used polymeric materials, and the blending of polyolefins is a common method to adjust and improve their properties. To understand the fundamental physics of polyolefins and their blends is significant to industrial applications and therefore received much attention in the past decades.[1–6] The proposing of spinodal crystallization mechanism,[7–11] although controversial, nevertheless has broaden the possible kinetics mechanism of crystallization of polyolefins. Furthermore, fluctuation-assisted crystallization mechanism[12] for a phase-separated blend is a milestone on the research of the interplay between the kinetics of liquid–liquid phase separation (LLPS) and crystallization in the polymer blend. In contrast to bulk systems, LLPS/crystallization interplay in thin films is very important to both fundamental physics and applications, while no work has been reported. Because of the interface effect and spatial confinement, phase separation and crystallization in blend films should be greatly different from that in the bulk. Surface enrichment of the component with lower surface energy often takes place to minimize the total surface energy of the system, which results to a surface-directed spinodal decomposition.[13–18]

In previous work,[12] simultaneous spinodal decomposition and crystallization in PEH/PEB blend system were studied systematically in bulk. The experimental results showed the overwhelming evidence of the concentration-fluctuation-assisted nucleation and the dominant results that most of the nucleation occurs at the interface. The mechanism of "fluctuation-assisted crystallization" was proposed to interpret the kinetics of such kind of the nucleation−crystallization process. As an important conclusion of that theory, nucleation rate after spinodal LLPS is proportional to the interfacial area in this polyolefin blend system. Therefore, when the domain size growing as $t^{1/3}$, the interfacial area decreases as $t^{-1/3}$, which results in the nucleation rate of subsequent crystallization decreases as $t^{-1/3}$, or more than $t^{-1/3}$ if the sharpening of the interphase was further accounted,[12] where t is the LLPS time.

In this Communication, the effect of the film thickness on the fluctuation-assisted crystallization was studied for the first time. The films of the PEH/PEB blend with the thickness of 800 and 400 nm were investigated, which is smaller or much smaller than the domain size in the late stage of spinodal decomposition in this case. And films with the thickness of 5 μm were also used for comparison. Combined reflection optical microscopy (OM) and scanning electron microscopy (SEM) results show that the effect of the LLPS time on nucleation rate of subsequent crystallization strongly depends on the film thickness. The surface segregation which causes additional interfacial area can be used to interpret the novel film thickness dependence of this fluctuation-assisted crystallization phenomenon of thin films.

The polyolefins used in this work are statistical copolymers of ethylene/hexane (PEH) (M_w = 110 kg/mol, 2 mol % hexene comonomer, $M_w/M_n \sim 2$) and ethylene/butene (PEB) (M_w = 70 kg/mol, 15 mol % butene comonomer, $M_w/M_n \sim 2$), supplied by ExxonMobil Co. Ltd. Since they were synthesized with metallocene catalysts, the samples have relatively narrow polydispersity ($M_w/M_n \sim 2$) and supposedly uniform statistically in comonomer distribution. PEH is the only crystallizable component of the PEH/PEB blend system above 60 °C. The blend of PEH and PEB with PEH mass fraction of 40% was prepared with the procedure same as that in the previous report.[12b] Silicon substrates were cleaned with piranha solution (H_2SO_4:H_2O_2 = 3:1) at 80 °C for 1 h, then rinsed in deionized water for several times, and dried with N_2 gas. (*Caution: piranha solution is hot and corrosive, and extreme care should be taken when handling this solution.*) The polymers were dissolved in *o*-xylene at 120 °C and then blade-coated onto preheated substrates. A custom-built flow coater similar to that in the literature[19] was used to control speed and height of the blade, which can produce well-controlled film thickness in a range of 200 nm−5 μm. The temperature of substrate was kept at 120 ± 1 °C by a custom-built PID-controlled hot stage fixed on the coater. The film thickness is measured by atomic force microscope (AFM) scrape test. All the blend films were melted at 160 °C for 60 min to eliminate thermal history before quenched to 135 °C for LLPS. After that, the samples were quenched to the crystallization temperature. All the heating processes were under N_2 atmosphere to avoid thermal degradation. Before SEM observation at lower secondary electron image mode (LEI, Jeol JSM-6700F), the films were etched with $KMnO_4/H_2SO_4/H_3PO_4$ solution to reveal the phase-separated structure.

The phase diagram of PEH/PEB in Figure 1 was cited from the literature,[20] and it shows that the PEH/PEB = 40/60 blend is within unstable region at 135 °C. SEM micrographs in Figure 2a,b displayed bicontinuous tubelike structure in blend films after heating at 135 °C for different times, which are characteristic of the late stages of spinodal decomposition. The domain

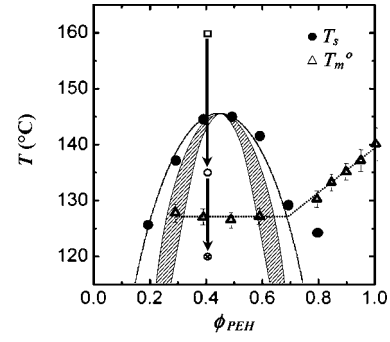

Figure 1. Phase diagram of PEB/PEH blends cited from ref 20. This diagram is used to indicate the LLPS temperature (○) and crystallization temperature (⊗) used in this report relative to the phase diagram of this blend system.

* To whom correspondence should be addressed: e-mail c.c.han@iccas.ac.cn, jzhao@iccas.ac.cn; tel +86-10-82618089, fax +86-10-62521519.
† State Key Laboratory of Polymer Physics and Chemistry.
§ Graduate University of the Chinese Academy of Sciences.

10.1021/ma7025379 CCC: $40.75
Published on Web 03/12/2008

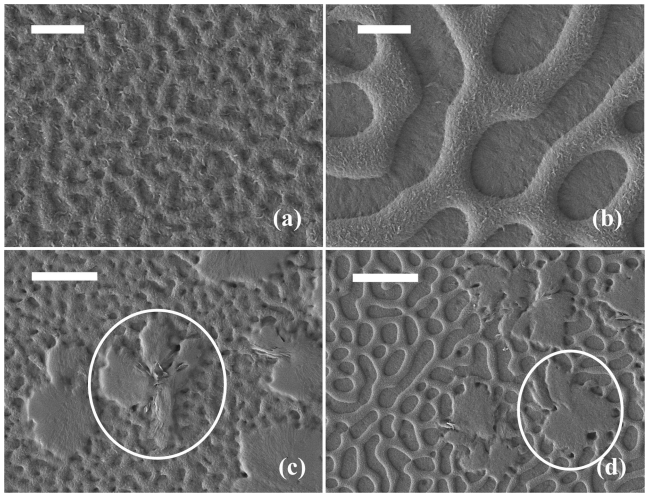

Figure 2. SEM micrographs (LEI mode) for PEH/PEB blend films with thickness of 800 nm after LLPS at 135 °C for (a) 0.5 h, (b) 6 h, and quenched in liquid N_2. (c) After LLPS at 135 °C for 0.5 h, crystallization at 120 °C for 15 min, and quenched in liquid N_2. (d) After LLPS at 135 °C for 6 h, crystallization at 120 for 15 min, and quenched in liquid N_2. Amorphous PEB-rich phase was removed by $KMnO_4/H_2SO_4/H_3PO_4$ solution. The scale bars in (a) and (b) correspond to 2 μm. The scale bars in (c) and (d) correspond to 5 and 10 μm, respectively.

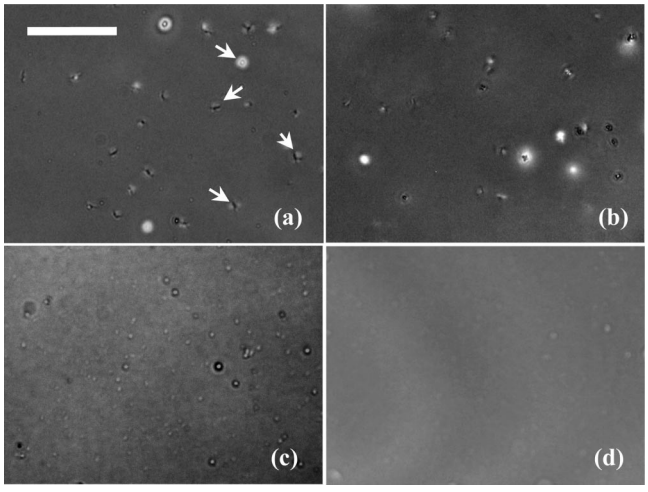

Figure 3. Reflection OM micrographs for PEH/PEB blend films with thickness of 400 nm (a, b) and 800 nm (c, d) after LLPS at 135 °C for 1 h (a, c) and 12 h (b, d) and then crystallization at 120 °C for 1000 s (a, b) and 500 s (c, d). The scale bar in (a) corresponds to 10 μm and also applies to (b)−(d). Arrows indicate some crystal in the films.

size grows from ca. 800 nm to 3 μm as the LLPS time increases from 0.5 to 6 h, which is close to and then exceeds the film thickness (800 nm) in this LLPS time scale. After the films were subsequently quenched to 120 °C, butterfly-like PEH crystals were found in the phase-separated blend films which was circled out in Figure 2c,d.

The nucleus increase in the films was recorded through in-situ reflection OM observation as shown in Figure 3. Both bright and dark dots in the photos are the crystalline grains. The difference in appearance resulted from different grain size and the focus of OM. The number of nuclei was counted in a viewing field of 320 × 240 μm^2. Then nucleation rates R during the early stage of crystallization can be obtained by linear fitting of the number of nuclei against the crystallization time t_c (Figure 4, insets). In the films with thickness of 800 nm (Figure 4b), for the first 6 h of LLPS, the relation between R and t are in accordance with a power law $R \sim t^{-\alpha}$, where the exponent α is

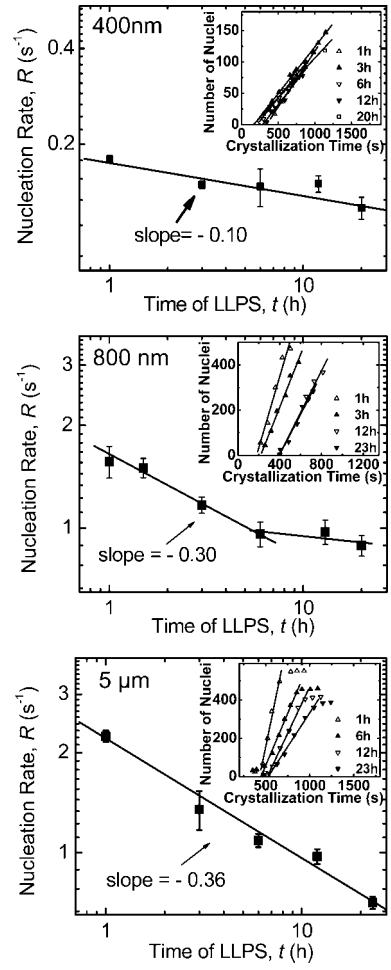

Figure 4. Nucleation rates in the PEH/PEB blend films at 120 °C after LLPS at 135 °C. The plots from top to bottom correspond to the films with thickness of (a) 400 nm, (b) 800 nm, and (c) 5 μm, respectively. Insets show the corresponding time evolution of nucleus number.

ca. 0.30. But for longer LLPS time, R does not change with t in an obvious manner. This critical LLPS time which started the very small or almost zero nucleation rate change is about 6 h for this 800 nm film thickness sample. In other words, as the domain size is growing (through LLPS) to a much larger dimension than the film thickness (about 4 times in this case), the nucleation rate becomes almost constant and independent of further LLPS. To further prove this phenomenon, crystallization rates in films with thickness of 400 nm were measured. This thickness is proved to be much smaller than the phase-separated domain size within the time scale of our recording. Results in Figure 4a shows the exponent α from linear fitting in the whole LLPS time scale in our experiment is only 0.10, which means that the changing of R is very small during LLPS time increasing from 1 to 20 h. The LLPS time is demonstrated to make little effect on the nucleation rate at this film thickness. For comparison and to make transition to bulk condition, nucleation rates in the films of 5 μm were measured (Figure 4c), which shows that R dependence on t are well represented with a power law. Linear fitting was obtained in the whole measured t range, and the corresponding α is calculated as −0.36, which is very close to the bulk data reported earlier.[12] The relations of R vs t at 120 °C in the blend films of different thickness are summarized in Figure 4, which reveals the distinct effect of film thickness on the LLPS time for the subsequence crystallization. It must be mentioned that all the rates of nucleation above are reported as nucleus increase per second,

which are commonly reported in events per second and per unit volume. Because of the fact that the sample measured in this case is not homogeneous along the thickness, the "nucleation rate" is defined differently in this paper just for the sake of comparison. For this case, the nucleation rate, R, is defined as the number of nucleation events per time, per viewing volume. The viewing volume is hA, where h is the film thickness and A is the area of viewing field, i.e., 7.68×10^4 μm^2 (320×240 μm^2) in this paper.

In the SEM pictures of the phase-separated films after etching process (Figure 2a,b), other than the bicontinuous structure, a rough layer was found to remain in the holes, which provided a key clue to interpret the above thickness dependence. Amorphous PEB-rich phase is dissolvable in the acid $KMnO_4$ etchant, while the PEH-rich phase can resist it for much longer time. This may be due that PEH crystallization during quenching made the molecules arranged more compactly in the PEH-rich phase compared with the PEB-rich phase, which can prevent the penetration of the etchant. Therefore, the remained layer is PEH-rich phase after the etching of PEB. The microgrooves morphology on this layer, which should correspond to the crystalline PEH, supported this conclusion further.

In a phase-separated mixture, surface is usually enriched by the component with lower surface energy, which can lead to surface-directed spinodal decomposition. Besides the chemical composition, the state of chain tension in the boundary layer can also affect surface energy of melt polymer. Although PEH and PEB possess almost the same chemical composition, lower density of side alkyl on PEH chain makes the chain more flexible, which could cause the attaching of PEH chain to the surface to lower polymer−substrate interfacial tension. As a result, from the very beginning[21] of the spinodal LLPS, a PEH-rich thin layer may have been formed on the silicon substrate.

Thus, the kinetics for the crystallization in the phase-separated polyolefin blend thin film can be interpreted as follows: The interfacial area between two separated phases is composed of two parts. One part is resulted from the surface-enriched layers of PEH, and the other part is from the bulk part of blend film. Changing LLPS time and film thickness does not change the quantity of the wetting layer. But the bulk layer of the film can go through the random spinodal LLPS. According to theoretical prediction[22–24] and the results in the bulk system,[12] the interfacial area of this part decrease by power law $t^{-\alpha}$, where the exponent α should be around 1/3 without accounting for the sharpening of the interphase. This part is greatly affected by film thickness. In thinner films, since the bulk part of the film is too thin to be a major contributor, surface layer becomes the dominating contributor. Interfacial area changes little according to the LLPS time, so does the nucleation rate. As the quantity of middle layer increases with the film thickness, its proportion in the total interfacial area also increases. When this part became dominating, the exponent α should gradually increasing from ca. 0 to 1/3. This film thickness effect should be relative to the ratio of the interfacial area contributed from the LLPS domains and from the total interface/surface area including the part covered by the surface-enriched PEH film. Thus, at a certain film thickness, taking 800 nm films as an example, the thickness is thick enough to keep the exponent α around 1/3 in the first 6 h of LLPS. While the domain size increases due to the coarsening of the spinodal decomposition process, the size of the phase-separated domains becomes much larger than the film thickness after LLPS time is lager than certain critical time (6 h in this case). The domains are deformed into pancakes shape, and the domain interface is only confined to the vertical walls of pancakes, which is greatly reduced compared to spherical domains dispersed in a continuous matrix. The surfaces of the films are covered by the PEH layers which are not changed. Therefore, the effect of the surface-enriched layers controls crystal nucleation process, which results in the insensitivity of nucleation rate with LLPS time.

In this report, we discussed the surface effect of thin film of PEH/PEB in order to interpret the effect of LLPS on the nucleation of crystallization process. The breakdown of dynamic scaling in thin film binary liquids undergoing phase separation has been reported before.[25] Bicontinuous domains grow with a decreasing exponent, 0.62 to 0.28, as the film thickness decreases from 900 to 90 nm in a dPMMA/SAN system. Although the wetting layer effect is strong enough and adequate to explain the varying exponent α for the nucleation process at a large region, further experiments[26] are necessary for quantifying the growth of the LLPS domains and the wetting layers for a detailed discussion of the critical LLPS time for the switch over of the nucleation mechanism as a function of the film thickness.

Again, in this study, the fluctuation-assisted crystallization in PEH/PEB blend films of thickness close to or less than the domain size of the spinodal decomposition was investigated by OM and SEM. The results show that the effect of the LLPS time on nucleation rate of subsequent crystallization strongly depended on the film thickness. In thicker films, where the film thickness is much large than the LLPS domain size, the nucleation rate decreases with LLPS time to the minus one-third power, $t^{-1/3}$, which is similar to that of bulk case. In thinner films, when the increasing domain size exceeded the film thickness, nucleation rate becomes insensitive to the LLPS time, t, gradually. Enriched layers of PEH were found on the film surfaces, which provide the physical explanation of this novel film thickness dependence of fluctuation-assisted crystallization.

Acknowledgment. The authors thank the financial support of Grants KJCX2-SW-H107, 2003CB615600, 20490220, 10590355, and 20634050.

References and Notes

(1) Hoffman, J. D. *Polymer* **1982**, *23*, 656.
(2) Hoffman, J. D.; Miller, R. L. *Macromolecules* **1988**, *21*, 3038.
(3) Klein, J.; Ball, R. *Discuss. Faraday Soc.* **1979**, *68*, 198.
(4) Lotz, B. *Eur. Phys. J. E* **2000**, *3*, 185.
(5) Dlugosz, J.; Fraser, G. V.; Grubb, D.; Keller, A.; Odell, J. A.; Goggin, P. L. *Polymer* **1976**, *17*, 471.
(6) Okada, M.; Nishi, M.; Takahashi, M.; Matsuda, H.; Toda, A.; Hikodaka, M. *Polymer* **1998**, *39*, 4535.
(7) Petermann, J.; Gohil, R. M.; Schultz, J. M.; Hendricks, R. W.; Lin, J. S. *J. Polym. Sci., Polym. Phys. Ed.* **1982**, *20*, 523.
(8) Imai, M.; Kaji, K.; Kanaya, T. *Macromolecules* **1994**, *27*, 7103.
(9) (a) Imai, M.; Mori, K.; Mizukami, T.; Kaji, K.; Kanaya, T. *Polymer* **1992**, *33*, 4451. (b) Imai, M.; Mori, K.; Mizukami, T.; Kaji, K.; Kanaya, T. *Polymer* **1992**, *33*, 4457.
(10) Terrill, N. J.; Fairclough, P. A.; Towns-Andrews, E.; Komanschek, B. U.; Young, R. J.; Ryan, A. J. *Polymer* **1998**, *39*, 2381.
(11) Olmsted, P. D.; Poon, W. C. K.; McLeish, T. C. B.; Terrill, N. J.; Ryan, A. J. *Phys. Rev. Lett.* **1998**, *81*, 373.
(12) (a) Zhang, X. H.; Wang, Z. G.; Muthukumar, M.; Han, C. C. *Macromol. Rapid Commun.* **2005**, *26*, 1285. (b) Zhang, X. H.; Wang, Z. G.; Dong, X.; Wang, D. J.; Han, C. C. *J. Chem. Phys.* **2006**, *125*, 024907.
(13) Jones, R. A. L.; Norton, L. J.; Kramer, E. J.; Bates, F. S.; Wiltzius, P. *Phys. Rev. Lett.* **1991**, *66*, 1326.
(14) (a) Puri, S.; Binder, K. *Phys. Rev. A* **1992**, *46*, R4487. (b) Puri, S.; Binder, K. *J. Stat. Phys.* **1994**, *77*, 145. (c) Puri, S.; Frisch, H. L. *J. Phys.: Condens. Matter* **1997**, *9*, 2109. (d) Binder, K. *J. Non-Equilib. Thermodyn.* **1998**, *23*, 1. (e) Binder, K.; Puri, S.; Frisch, H. L. *Faraday Discuss.* **1999**, 103. (f) Puri, S.; Binder, K. *Phys. Rev. Lett.* **2001**, *86*,

1797. (g) Puri, S.; Binder, K. *Phys. Rev. E* **2002**, *66*, 10. (h) Puri, S. J. *J. Phys.: Condens. Matter* **2005**, *17*, R101.
(15) Kim, E.; Krausch, G.; Kramer, E. J.; Osby, J. O. *Macromolecules* **1994**, *27*, 5927.
(16) Chen, H.; Chakrabarti, A. *Phys. Rev. E* **1997**, *55*, 5680.
(17) Geoghegan, M.; Ermer, H.; Jungst, G.; Krausch, G.; Brenn, R. *Phys. Rev. E* **2000**, *62*, 940.
(18) (a) Wang, H.; Composto, R. J. *Phys. Rev. E* **2000**, *61*, 1659. (b) Wang, H.; Douglas, J. F.; Satija, S. K.; Composto, R. J.; Han, C. C. *Phys. Rev. E* **2003**, *67*, 6.
(19) (a) Meredith, C.; Karim, A.; Amis, E. J. *Macromolecules* **2000**, *33*, 5760. (b) Smith, A. P.; Douglas, J. F.; Meredith, C.; Amis, E. J. ; Karim, A. *J. Polym. Sci., Part B: Polym. Phys.* **2001**, *39*, 2141.
(20) Wang, H.; Shimizu, K.; Hobbie, E. K.; Wang, Z. G.; Meredith, J. C.; Karim, A.; Ami, E. J.; Hsiao, B. S.; Hsieh, E. T.; Han, C. C. *Macromolecules* **2002**, *35*, 1072.
(21) Surface segregation has also been proposed for a polymer blend prior to the phase separation in the bulk, for the segregation can lower the overall free energy of the system: Henderson, I. C.; Clarke, N. *Macromol. Theory Simul.* **2005**, *14*, 435.
(22) Lifshitz, I. M.; Slyozov, V. V. *J. Phys. Chem. Solids* **1961**, *19*, 35.
(23) Binder, K.; Stauffer, D. *Phys. Rev. Lett.* **1974**, *33*, 1006.
(24) Tanaka, H. *J. Chem. Phys.* **1996**, *105*, 1099.
(25) Chung, H. J.; Composto, R. J. *Phys. Rev. Lett.* **2004**, *92*, 4.
(26) Studies in progress.

MA7025379